ISSN: 1999-6691, e-ISSN: 2782-3709 DOI: http://doi.org/10.7242/1999-6691/2024.17.1.3

Research article

Pulsations of the liquid metal flow generated by an alternating magnetic field

A.O. Poluyanov, I.V. Kolesnichenko

Institute of Continuous Media Mechanics UB RAS, Perm, Russian Federation

This paper studies numerically a vortex flow of liquid metal driven by an electromagnetic force, which is generated by the interaction of the alternating magnetic field of a short solenoid with the induced electrical current. A short solenoid is placed coaxially in a cylindrical cell at half of its height. The mathematical model used to describe the process is based on the equations of magnetic hydrodynamics in the induction-free approximation. Calculations, which are carried out by the control volume method using the ANSYS Fluent package, show that the average flow has the form of two toroidal vortices. The calculated velocity fields are indicative of the pulsating behavior of vortices, accompanied by a change in their sizes. In the examined range of the force parameter, the predominant flow pattern is the single-mode pulsation flow. The dependence of the characteristic frequency and Reynolds number on the force parameter are obtained using spectral analysis. It has been found that the period of pulsations is close to the period of rotation of a large-scale vortex. It has been established that the pulsations are of quasi-periodic character, and a distinct pulsation frequency is observed only in the flow region near the solenoid. The effect of velocity pulsations is strong and can be detected in the laboratory experiment with gallium eutectic. The performance of such experiment is planned for the near future. The flow rate of gallium eutectic will be measured by an ultrasonic Doppler velocimeter. The results of numerical modeling and their verifications can be useful in determining the ways of reducing the intensity of vortex flows during the electromagnetic separation of impurities, which is based on the induction mechanism responsible for the generation of electromagnetic force that displaces particles. The data on the pulsation frequency of the unsteady flow can be used in the development of a non-contact technique for estimating the average electrical conductivity of a two-phase medium, such as liquid metal with undesirable impurities.

Keywords: magnetic hydrodynamics, alternating magnetic field, electromagnetic force, vortex flow, azimuthal pinch, numerical modeling, ANSYS Fluent package

Received: 28.09.2023 / *Published online*: 01.04.2024

1. Introduction

The method of non-contact generation of liquid metal flow has been widely used for many years in the production processes of metallurgy [1] and power engineering [2] associated with high temperature melts (in metallurgy) and liquid-metal coolants (at nuclear power plants), which are chemically aggressive. The non-contact method has a number of advantages compared to mechanical action on liquid metal. Thus, with the help of an alternating magnetic field a vortex flow is excited, i.e. an induction mechanism of electromagnetic force generation is realized. The appearance of the vortex electromagnetic force is explained by the fact that the alternating magnetic field of the solenoid generates a vortex electric current in the electrically conductive medium due to electromagnetic induction. This current in turn generates its own magnetic field. The interaction of the current and the resulting magnetic field leads to the appearance of the electromagnetic force [3]. One system that is often used as a basis both in scientific research and in applications is a cylindrical cell with liquid metal, which is coaxially placed in a cylindrical solenoid through which an alternating electric current. This configuration, by analogy with plasma physics, has been called "azimuthal pinch". In practice, it and its variants, in addition to tokamaks (toroidal chambers with magnetic coils), are most commonly used in induction furnaces [3], electromagnetic stirrers [4, 5], and electromagnetic pumps [6, 7].

Electromagnetic force and vortex flow have a selective effect on liquid electrically conductive multiphase media [8, 9]. This effect is realized in electromagnetic separators [10–12], which are designed to extract solid inclusions from molten melts. The purification of liquid metals is an urgent task for both metallurgical [8] and nuclear [2] industries. In [9–12], consideration is given to a conduction mechanism of electromagnetic force generation in a separator, when direct or alternating current initially flows through a cell exposed to a magnetic field. The disadvantage of the conduction mechanism is the engineering difficulty of supplying the electric current to the cell. Therefore, to realize the separation effect, the induction mechanism of electromagnetic force generation through the use of a solenoid has also been the focus of intensive study [13–15]. The disadvantage of this method is the appearance of a vortex mixing flow [15], the undesirable influence of which must be reduced. This can be accomplished by using information on the characteristics of these flows.

The behavior of a liquid metal flow in the "azimuthal pinch" configuration is studied in detail in the framework of induction melting problems both experimentally [16, 17] and numerically [17–19] in the case when the cell height is less than the solenoid height. The appearance of pulsations flow regimes with both free upper boundary [16] and closed

boundary [17–19] has been detected. Pulsations of the flow lead to pulsations of the impurity distribution field [19], which plays an important role in the process of electromagnetic separation. However, the results of these works do not allow us to answer a number of questions, which are the subject of the study in this article.

The aim of the work is to characterize the pulsations modes of flows caused by the action of the alternating magnetic field of a short solenoid, the height of which is significantly less than the height of the cell. It is also important to clarify how the frequency of pulsations f behaves in the region of the cell, and whether the pulsations are harmonic or have a more complex spectral composition. Finally, it is necessary to find out how the pulsation frequency depends on the intensity of the electromagnetic force action and what mechanism governs this dependence. Also, under consideration is the possibility of measuring the characteristic frequency of the velocity pulsation, which can form the basis for diagnostics of the properties of the examined electrically conductive medium. The study is carried out by mathematical modeling. It should be noted that modeling of processes in liquid metals, especially with the prospect of involvement of thermophysical processes, requires special efforts to develop and verify the mathematical models [20]. Therefore, an additional motivation is to obtain an assessment of the possibility of implementation of the verification experiment.

2. Problem Statement and Methods

So, we study the flow of liquid metal in a cylindrical cell *1* (Fig. 1*a*), which is oriented vertically. In the case of a short solenoid *2*, it generates a poloidal alternating magnetic field. This field in turn induces an azimuthal field of the eddy electric current in liquid metal. The resulting electric current of density $\mathbf{j}$ has its own eddy poloidal magnetic field. The superposition of the magnetic fields is found as a product of the frequency by electrical conductivity of the medium, and the larger is its magnitude, the smaller is the amplitude of electromagnetic waves as they penetrate deeper into the conducting medium (skin effect). In the proposed formulation, the parameters of the problem are such that the region of the highest values of the magnetic field and electric current density is localized near the solenoid. Moreover, in this region, the vertical component of the magnetic field significantly exceeds its radial component. Because of this, the electromagnetic force $\mathbf{f}^{em}$ arising from the interaction between the azimuthal current and the vertical component of the intrinsic magnetic field will have predominantly a radial component. Thus, in the region near the solenoid, the electromagnetic force acts in the radial direction from the periphery to the axis of the cylinder, i.e., the described system, consisting of a cylindrical cell with liquid metal and coaxially located cylindrical solenoid, behaves like the "azimuthal pinch" observed in plasma physics [17]. In this system, the squeezing forces are called "pinch" forces. For a short solenoid, the maximum value of the force in the axial direction is observed in the solenoid region at midway along the cylinder length and decreases towards the ends. The electromagnetic force is potential only for infinitely long cylinders and solenoids. In the system under consideration, the vector field of the electromagnetic force will be vortex, which inevitably gives rise to a vortex flow of the conducting fluid. The distinguishing features of this flow is investigated further.

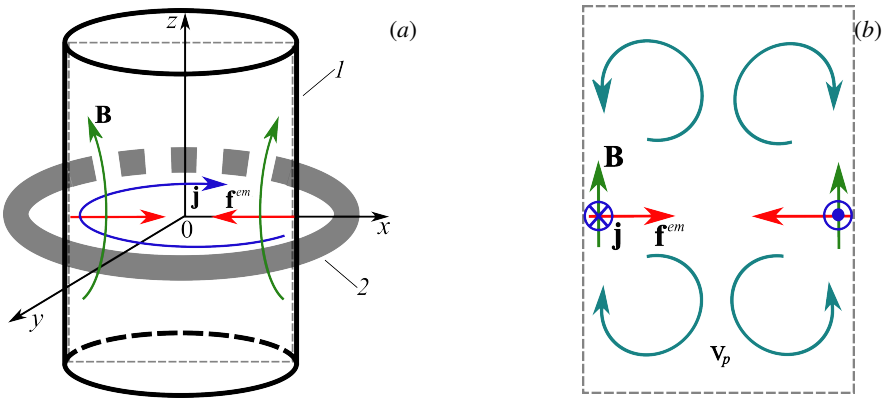

Fig. 1. Schematic representation of the problem formulation (*a*): cylindrical cell *1*, solenoid *2*; acting in the longitudinal axial section of the computational field domain (*b*), in which the instantaneous directions of the current density $\mathbf{j}$ and induction $\mathbf{B}$ of the intrinsic magnetic field at the periphery of the cell near the solenoid are shown, as well as the direction of the force $\mathbf{f}^{em}$ and field v_p

The developed vortex flow has a dominant poloidal component v_p of the velocity vector field $\mathbf{v}$ (Fig. 1*b*). It means that these velocity components lie in meridional planes. The azimuthal velocity component is initially absent, but may

appear as a result of the development of flow pulsations.

The presence of the eddy current leads to the local heating of liquid metal, which can cause a convective flow. The velocity of this flow is expected to be much less than the velocity of the flow caused by the electromagnetic force. Thus, in work [21], where the convection of liquid sodium in a cylindrical cell was studied experimentally, the velocity of large-scale circulation was 0.06 m/s, which required that the temperature difference between the cylinder ends should be equal to 30°C. In the problem under study, the geometric and physical conditions for the development of such a flow are less favorable. Moreover, the stirring current equalizes the temperature in the cell and generally alters the conditions for the generation of the Rayleigh-Benard convection. Therefore, convection was not considered in this work.

The main flow can produce both desirable and undesirable effects. In order to strengthen or weaken the accompanying effects, it is necessary to get information about its modes and parameters to be able to use it to influence the process in the cell-solenoid system. In this paper, the vortex flow is studied by mathematical modeling. The model is formulated on the basis of the equations of magnetic hydrodynamics in the electrodynamic approximation [7]:

$$\nabla\times\frac{\mathbf{B}}{\mu_0}=\mathbf{j},\quad \nabla\times\mathbf{E}=-\frac{\partial\mathbf{B}}{\partial t},\tag{1}$$

$$\nabla\cdot\mathbf{B}=0,\quad \nabla\cdot\mathbf{E}=0,\tag{2}$$

$$\mathbf{j}=\sigma\mathbf{E},\tag{3}$$

$$\mathbf{f}^{em}=\mathbf{j}\times\mathbf{B},\tag{4}$$

$$\frac{\partial\mathbf{v}}{\partial t}+(\mathbf{v}\cdot\nabla)\mathbf{v}=-\frac{1}{\rho}\nabla p+\nu\triangle\mathbf{v}+\frac{1}{\rho}\mathbf{f}^{em},\tag{5}$$

$$\nabla\cdot\mathbf{v}=0.\tag{6}$$

Such representation allows us to solve separately the problems of electrodynamics and hydrodynamics. The result of solving the electrodynamics problem described by Maxwell's equations (1), (2), and Ohm's equations (3) is the electromagnetic force, acting on the conducting fluid $\mathbf{f}^{em}$ (4). In the hydrodynamic problem, the evolution of the fluid flow velocity $\mathbf{v}$ is determined from the solution of the Navier-Stokes equation (5) and the continuity equation (6). The equations (1)–(6) also adopt the following notation: $\triangle$ — Laplace operator; $\mathbf{B}$ — magnetic field induction; $\mathbf{j}$ — current density; $\mathbf{E}$ — electric field strength; t — time; μ_0 — magnetic constant; σ — electric conductivity; ν — kinematic viscosity; ρ — density of liquid metal. The square of the Hartmann number $\mathrm{S}=\mathrm{Ha}^2=\sigma B_0^2 d^2/(\rho\nu)$ containing B_0 , which is the maximum value of the magnetic field induction in the area of the cell is taken as a dimensionless criterion S (force parameter) that will be used further to generalize the results. The criterion S does not contain the frequency f, so that the results are also valid for its fixed value, which in this study was assumed to be equal to $f_e=120$Hz. The criterion S appears in the Navier-Stokes equation as a result of nondimensionalization of the (1)–(6) equations when the following quantities are taken as characteristic parameters: the cell diameter d is taken for a distance, ν/d - for velocity, d^2/ν -for time, B_0 -for magnetic field, $\sigma B_0\nu/d$ - for current density. The criterion S characterizes the ratio of electromagnetic forces to viscous forces.

The solution of the electrodynamic part of the problem is carried out in the domain divided into subdomains containing, respectively, a cell with liquid metal, a solenoid, and air. The magnetic permeability of all subdomains is assumed to be equal to unity, so there are no changes in magnetic induction during the transition between subdomains. The vector component of the eddy electric current density, which is normal to the boundary of the subarea with liquid metal, is zero. The azimuthal component of the current density in the solenoid is prescribed.

The solution of the hydrodynamic part of the problem is searched for in the subdomain containing liquid metal. On the lateral and end surfaces of the subdomain, the no-slip condition is fulfilled: $\mathbf{v}=0$.

Since the study is carried with a view to perform an experiment, it is necessary to specify the physical and geometrical characteristics of the system. Thus, the cylindrical cell is filled with a eutectic alloy (gallium, stannum, zincum), the properties of which are well known [22]. Thus, at room temperature its density is $\rho=6150$ kg/m^3, kinematic viscosity is $\nu=2.9\cdot10^{-7}$m^2/s, and electrical conductivity is $\sigma=2.6\cdot10^6$ Sm/m. The height of the cylindrical cell is 0.100 m, the radius is 0.038 m. The short solenoid *2* has a height of 0.02 m, an inner radius of 0.048 m, an outer radius of 0.138 m; the solenoid consists of two layers with a gap of 0.006 m between them. The number of turns in each layer of copper wire with a cross section of 0.007×0.001 m is 132. A series of calculations have been performed for the frequency of the current in solenoid $f_e=120$ Hz. The maximum absolute value of the magnetic field induction B_0 varies in the range from numerical 0.015 to 0.03 T.

The numerical implementation is done using the ANSYS Emag package (electrodynamic part) and ANSYS Fluent with the user-defined UDF function (hydrodynamic part). The time step is $h_t = 0.01$ s, the hydrodynamic grid step is $h_d = 0.003$ m. The Reynolds numbers in the simulated flows are of the order of $\mathrm{Re} \approx 10^4$. The large eddy simulation (LES) method is used to describe turbulence. An important condition in the fluid dynamics problems is the Courant condition $h_t \nu / h_d < C$; here it is assumed that the constant $C < 1$.

All calculations start from the rest state. At each time step, the velocity field is kept unchanged and the kinetic energy of the poloidal and azimuthal (toroidal) velocity components is calculated in the same way as in the study of similar flows in [23]:

$$E_{\mathrm{pol}} = \frac{\rho}{2} \int\limits_V \left(\mathrm{v}_r^2 + \mathrm{v}_z^2\right) dV, \quad E_{\mathrm{az}} = \frac{\rho}{2} \int\limits_V \mathrm{v}_\varphi^2 dV.$$

3. Results

Analysis of the evolution of three-dimensional velocity fields and their two-dimensional projections onto the longitudinal axial planes has shown that in the range of parameters studied, the flow development can be divided into two stages. At the first stage, the kinetic energy grows to some maximum value. At the second stage, there is a transition of energy to a stationary state accompanied by the appearance of a pulsations flow. At both stages, the development of three-dimensional flow consisting of two toroidal vortices is observed. The components of the flow velocity vector lie mainly in the meridional plane. The average fields of the poloidal velocity component in the longitudinal axial cross section are plotted based on the results of the calculations (Fig. 2*a*). The averaging was carried out at the second stage of the flow. The smallness of the azimuthal velocity component is confirmed by the fact that the poloidal component of the kinetic energy significantly exceeds its azimuthal component (Fig. 2*b*), which is associated with the velocity pulsations. Note that the poloidal velocity pulsations significantly exceed the azimuthal velocity pulsations. At the second stage, the migration of large-scale vortices across the area of the cell takes place. The pulsations regime is of steady-state character, which can be seen from the evolution of the kinetic energy (Fig. 2*b*), where the dashed line shows the mean value. The calculation lasted for 500 s of physical time. The choice of such computation time was dictated by the fact that it was found to be sufficient for calculating the characteristics of the pulsations.

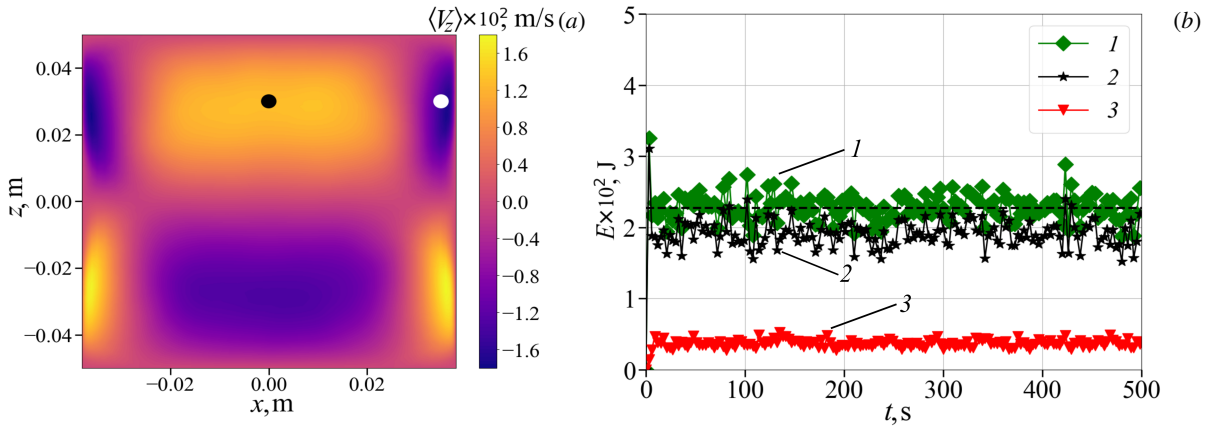

Fig. 2. Time-averaged results for solenoid with current strength $I = 20$A and frequency $f_e = 120$Hz: vertical velocity component field in the vertical axial section (*a*); evolution of flow kinetic energy and its components (*b*)

The value of the hydrodynamic Reynolds number $\mathrm{Re} = V_z R / \nu$ was determined by solving the problem based on the average velocity V_z in equilibrium, the cell radius R, and the kinematic viscosity ν. The velocity V_z was averaged in the regions of the cell marked with black and white dots as shown in 2*a*. The choice of dots depended on the shape of the vortex flow.

Typically, the pulsations are estimated by the velocity dependence at some point within the cell. One-dimensional velocity signals were also analyzed, i.e., a function $\mathbf{v}(t)$ was found. In order to avoid searching through all points in the cell, the velocity profile diagrams were preliminary plotted. For this purpose, the velocity profiles obtained at each

time step were plotted sequentially within the specified computation time (Fig. 3). Both the visual and quantitative velocity estimation was performed using a color scale. The velocity profiles were obtained only for the vertical component of the velocity $V_z(x,0,z)$, with only two values taken for demonstration in the direction of the x-axis, m: 0 and 0.035. This is due to the fact that at the next stage it is planned to conduct an experimental study of the described process using sensors of the ultrasonic Doppler velocimeter (UDV). They will be placed at these points and will allow the evolution of the velocity projection profile to be recorded in the direction of the emitted ultrasonic beam [24]. Figure3*a* shows the evolution of the velocity pulsations along the cell.

Analysis of the diagrams over the entire time interval showed that at the initial moment the flow is localized in the inductor region, in which its intensity reaches the highest value. As the flow evolves, it spreads over a larger volume of the channel, with the maximum value of its velocity slightly decreasing. The diagrams constructed for the second (pulsations) mode confirm the presence of pulsations (Fig. 3). It can be seen that at $x=0$ the intensity of pulsations along the axis of the cell increases in the region of the highest values of velocity, while in the central plane $z=0$ there is a region of less intense flow and, consequently, weak pulsations (Fig. 3*a*). Near the wall ($x=0.035$ m), the picture changes: in the central part of the channel the pulsations are more intensive and accompanied by a change in the flow direction (Fig. 3*b*). It is seen that the pulsations are not strictly regular, especially near the wall.

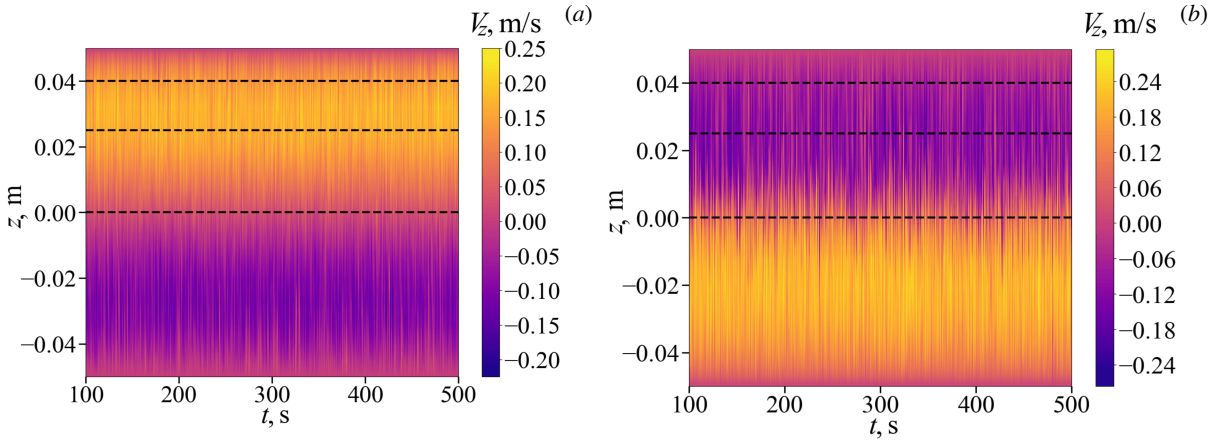

Fig. 3. Profiles of the vertical velocity component at $x=0$ m (*a*) and $x=0.035$ m (*b*); solenoid with current strength $I=20$A and frequency $f_e=120$Hz

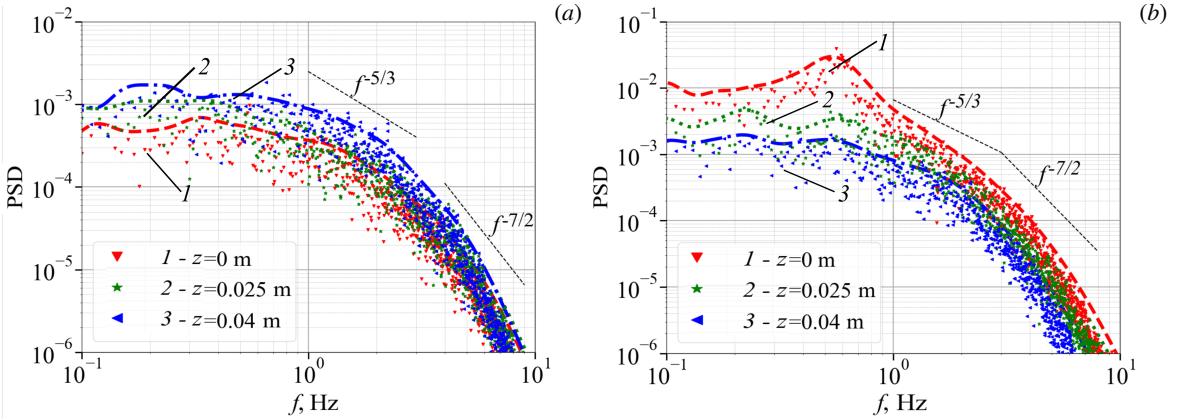

Fig. 4. Fourier and wavelet spectra of signals for central (*a*) and near-wall (*b*) profiles of the vertical velocity component; solenoid with current strength $I=20$A and frequency $f_e=120$Hz

To determine the characteristic frequency of velocity pulsations in the power spectral density (PSD)-frequency coordinates, the Fourier spectra (Fig. 4) are constructed for the selected velocity profile at points, whose positions are shown by dashed lines in 3. Since in general the pulsations are of irregular nature, the spectral composition of the velocity

signal at a point in space changes with time. Therefore, the wavelet transform [25] based on the Morlet wavelet was used to find the characteristic frequencies of the pulsations. In 4, the Fourier spectra are marked by triangles, and the integral wavelet spectra of the same signals - by dashed lines. The results indicate that there is a point in the near-wall profile (Fig. 2*a*) that demonstrates the presence of the characteristic pulsations frequency. Most of the other points do not have a pronounced characteristic pulsations frequency. Similar results have been obtained for flows at different values of the force parameter S. For the sake of visualization, the slopes of the spectra are labeled "–5/3" and "–7/2". The numbers *1*, *2*, *3* denote spectra corresponding to different values of the coordinate z.

The nature of the pulsations is best demonstrated by the wavelet spectrograms of velocity pulsations (Fig. 5). They make it possible to trace changes in the structure of flow pulsations with time, which is impossible to do with Fourier spectra. The absence of dominant horizontal structures suggests in general the absence of regular pulsations of a given frequency (Fig. 5*a*). The well-defined horizontal structures of high intensity on the spectrogram correspond to some predominant frequency in the signal. There can be several horizontal structures,which is indicative of the presence of several frequencies. In this case, the structures elongated relative to others are observed in the middle part of the spectrogram and confirm the observation that pulsations with frequencies lying in the interval 0.4–0.6 Hz (Fig. 5*b*) often occur in the near-wall region of the flow for a given value of the force parameter $\mathrm{S} = 3.4 \times 10^4$.

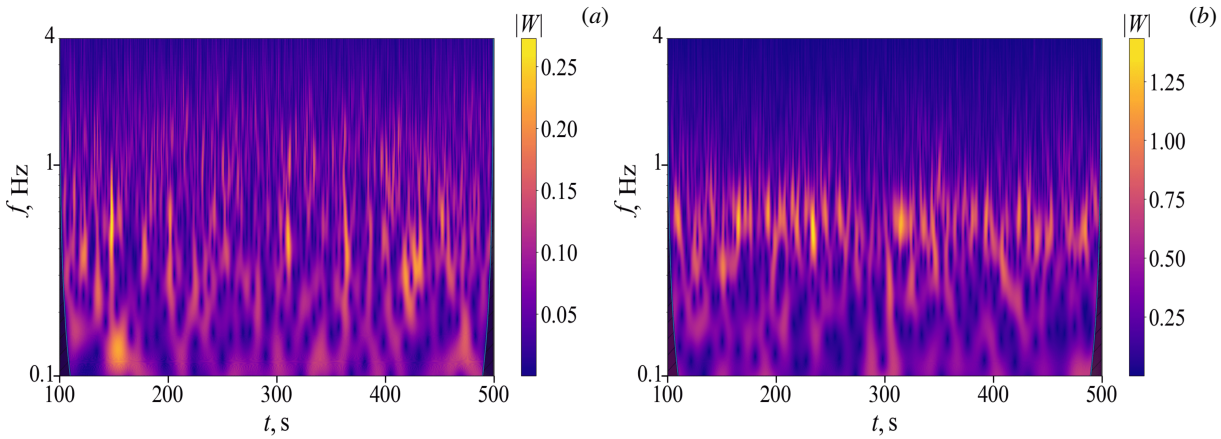

Fig. 5. Wavelet spectrograms of velocity signals at the point $z = 0$ for central (*a*) and near-wall (*b*) velocity profiles; solenoid with current strength $I = 20$A and frequency $f_e = 120$Hz

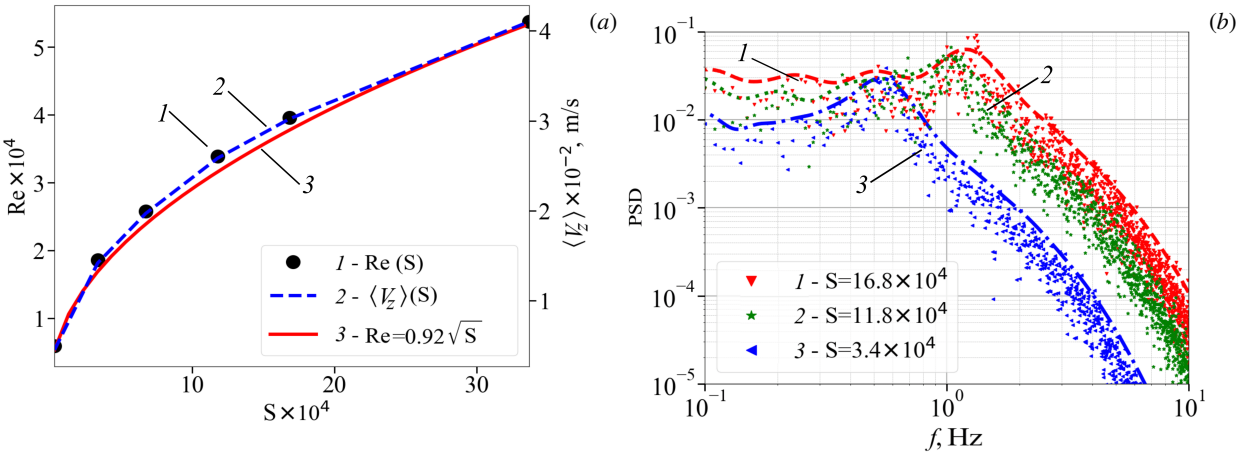

Fig. 6. Mean velocity and Reynolds number as the functions of the dimensionless force parameter S (shown for the near-wall region, see white dot in Figure 2*a*) (*a*); Fourier spectra at a fixed point for different values of the force parameter in solenoid with current strength $I = 20$ A and frequency $f_e = 120$ Hz (*b*)

In order to elucidate how the characteristic frequency of pulsations changes depending on the magnitude of the force

parameter, the corresponding graph is plotted. The most rational way to analyze the intensity of the flow is to apply to the values obtained in the region of its highest velocity (see Fig. 2, black and white points). The Reynolds number was found to be related to the force parameter by the square root law (Fig. 6*a*). Presumably, the velocity growth is hampered by increased turbulization of the flow, which leads to increased dissipation. The absence of curve inflections indicates that the additional large-scale flow modes are not formed in the investigated range of the force parameter. The fragment of 6*a* also shows a velocity scale for quantitative assessment of the magnitude of the characteristic flow intensity.

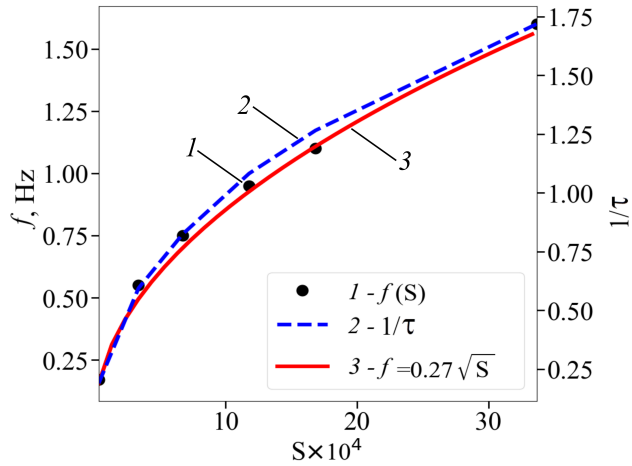

Fig. 7. The dependence of the characteristic frequency on the force parameter; solenoid with current strength $I = 20$ A and frequency $f_e = 120$ Hz

Analysis of the velocity spectra at the white point of the near-wall region (Fig. 2*a*) obtained for different values of the force parameter showed that after the linear growth, the characteristic frequency of pulsations increases nonlinearly and is accompanied by an increase in the intensity of pulsations (Fig. 6*b*). It turned out that the dependence of the characteristic frequency of the flow velocity pulsations on S also obeys the square root law (Fig. 7). This confirms the absence of additional pulsations modes of the highly intensive flow. In the same figure, the scale of the parameter τ , which is the estimated time of one revolution of a large-scale poloidal vortex, is shown on the right. The inverse value characterizes the frequency of vortex turnover.

4. Conclusions

The numerical study of the vortex flow in a cylindrical cell has shown that pulsations modes occur in the examined range of parameters. The analysis of the spatial structure of the flow allowed us to conclude that the main mode of the large-scale circulation consists of two toroidal vortices, which are clearly visible in the averaged velocity field diagrams. Such velocity field patterns are characteristic of the flow obtained under the action of an alternating magnetic field in the studies by other authors (see, for example, [17, 18]).

The velocity pulsations observable in the instantaneous fields are due to the generation of the pulsations mode of the flow, the scale of which is smaller than the scale of the main mode. The application of the Fourier analysis allowed us to detect the selected frequency, and wavelet analysis was used to estimate its magnitude. Wavelet spectrograms demonstrated that the pulsations mode with this frequency does not occur continuously, but a certain number of times per unit time. This frequency was found to be comparable to the frequency of turnover of a large-scale poloidal vortex (see Fig. 7). Similar results were obtained for convective large-scale circulation in [21–26]. The dependence of the characteristic frequency of pulsations on the force parameter S is of the same form as the Reynolds number dependence. The absence of inflection points on this curve suggests that one mode of large-scale circulation in the parameter range under consideration is predominant.

The spatial analysis of pulsations showed that this characteristic frequency cannot be reliably detected at all points of the cell. The best result was obtained for the point located in the near-wall region. It is just the region to which the maximum electromagnetic force corresponds. This gives hope for the possibility of recording the characteristics of pulsations on the basis of accurate measurement of the winding supply parameters in the future gallium eutectic experiment with application of an ultrasonic Doppler velocimeter. This will make it possible to verify the mathematical

model of this process through further development of research described in this paper. The results obtained provide a basis for the improvement of noninvasive techniques for operative control of some liquid metal properties. Finally, reliable information on the flow modes arising in the near wall regions of a solenoid of any length opens the way for developing methods to reduce the undesirable influence of the stirring flow on the process of electromagnetic separation.

The research was carried out at the expense of the grant of the Russian Science Foundation and the Perm Region № 22-19-20106, https://rscf.ru/project/22-19-20106/.

References

1. *Povkh I.L.*, *Kapusta A.B.*, *Chekin B.V.* Magnitnaya gidrodinamika v metallurgii. Moscow: Metallurgiya, 1974. 240 p.
2. *Arkhipov V.M.* Tekhnika raboty s natriyem na AES. Moscow: Energoatomizdat, 1986. 136 p.
3. *Tarapore E.D.*, *Evans J.W.* Fluid velocities in induction melting furnaces: Part I. Theory and laboratory experiments. Metallurgical Transactions B. 1976. Vol. 7, no. 3. P. 343–351. DOI: 10.1007/bf02652704.
4. *Moffatt H.K.* Electromagnetic stirring. Physics of Fluids A: Fluid Dynamics. 1991. Vol. 3, no. 5. P. 1336–1343. DOI: 10.1063/1.858062.
5. *Denisov S.*, *Dolgikh V.*, *Khripchenko S.*, *Kolesnichenko I.*, *Nikulin I.* The effect of traveling and rotating magnetic fields on the structure of aluminum alloy during its crystallization in a cylindrical crucible. Magnetohydrodynamics. 2014. Vol. 50, no. 4. P. 407–422. DOI: 10.22364/mhd.50.4.8.
6. *Vol'dek A.* Induktsionnyye magnitogidrodinamicheskiye mashiny s zhidkometallicheskim rabochim telom. Leningrad: Energiya, 1970. 271 p.
7. *Kolesnichenko I.*, *Khalilov R.* Extremum in the dependence of the head generated by electromagnetic pump of liquid metal on feeding current frequency. Computational Continuum Mechanics. 2022. Vol. 15, no. 4. P. 495–506. DOI: 10.7242/1999-6691/2022.15.4.38.
8. *Povkh I.L.*, *Chekin B.V.* Magnitogidrodinamicheskaya separatsiya. Kiyev: Naukova dumka, 1978. 148 p.
9. *Kolesnichenko I.* Investigation of electromagnetic force action on two-phase electrically conducting media in a flat layer. Magnetohydrodynamics. 2013. Vol. 49, no. 1. P. 217–222. DOI: 10.22364/mhd.
10. *Mamykin A.*, *Losev G.*, *Kolesnichenko I.* Model of electromagnetic purification of liquid metal. Magnetohydrodynamics. 2021. Vol. 57, no. 1. P. 73–84. DOI: 10.22364/mhd.
11. *Kolesnichenko I.V.*, *Mamykin A.D.*, *Losev G.L.* Device for cleaning molten metal and electrolytes from impurities. 2019. RF Patent No. 2,681,092, Byull. Izobret., 4 April 2019.
12. *Xu Z.*, *Li T.*, *Zhou Y.* Continuous Removal of Nonmetallic Inclusions from Aluminum Melts by Means of Stationary Electromagnetic Field and DC Current. Metallurgical and Materials Transactions A. 2007. Vol. 38, no. 5. P. 1104–1110. DOI: 10.1007/s11661-007-9149-y.
13. *Taniguchi S.*, *Brimacombe J.K.* Application of Pinch Force to the Separation of Inclusion Particles from Liquid Steel. ISIJ International. 1994. Vol. 34, no. 9. P. 722–731. DOI: 10.2355/isijinternational.34.722.
14. *Zhang B.*, *Ren Z.*, *Wu J.* Continuous electromagnetic separation of inclusion from aluminum melt using alternating current. Transactions of Nonferrous Metals Society of China. 2006. Vol. 16, no. 1. P. 33–38. DOI: 10.1016/S1003-6326(06)60006-X.
15. *Shu D.*, *Sun B.*, *Li K.*, *Wang J.*, *Zhou Y.* Effects of Secondary Flow on the Electromagnetic Separation of Inclusions from Aluminum Melt in a Square Channel by a Solenoid. ISIJ International. 2002. Vol. 42, no. 11. P. 1241–1250. DOI: 10.2355/isijinternational.42.1241.
16. *Galpin J.M.*, *Fautrelle Y.* Liquid-metal flows induced by low-frequency alternating magnetic fields. Journal of Fluid Mechanics. 1992. Vol. 239. P. 383–408. DOI: 10.1017/S0022112092004452.
17. *Cramer A.*, *Galindo V.*, *Zennaro M.* Frequency dependence of an alternating magnetic field driven flow. Magnetohydrodynamics. 2015. Vol. 51, no. 1. P. 133–148. DOI: 10.22364/mhd.51.1.13.
18. *Umbrashko A.*, *Baake E.*, *Nacke B.*, *Jakovics A.* Modeling of the turbulent flow in induction furnaces. Metallurgical and Materials Transactions B. 2006. Vol. 37. P. 831–838. DOI: 10.1007/s11663-006-0065-0.
19. *Ščepanskis M.*, *Jakovičs A.*, *Baake E.*, *Nacke B.* Analysis of the oscillating behaviour of solid inclusions in induction crucible furnaces. Magnetohydrodynamics. 2012. Vol. 48, no. 4. P. 677–686. DOI: 10.22364/mhd.48.4.8.

20. *Rogozhkin S.*, *Aksenov A.*, *Zhluktov S.*, *Osipov S.*, *Sazonova M.*, *Fadeyev I.*, *Shepelev S.*, *Shmelev V.* Development and verification of a turbulent heat transport model for sodium-based liquid metal coolants. Computational Continuum Mechanics. 2014. Vol. 7, no. 3. P. 306–316. DOI: 10.7242/1999-6691/2014.7.3.30.

21. *Khalilov R.*, *Kolesnichenko I.*, *Pavlinov A.*, *Mamykin A.*, *Shestakov A.*, *Frick P.* Thermal convection of liquid sodium in inclined cylinders. Physical Review Fluids. 2018. Vol. 3, no. 043503. DOI: 10.1103/physrevfluids.3.043503.

22. *Dobosz A.*, *Plevachuk Y.*, *Sklyarchuk V.*, *Sokoliuk B.*, *Gancarz T.* Thermophysical properties of the liquid Ga–Sn–Zn eutectic alloy. Fluid Phase Equilibria. 2018. Vol. 465. P. 1–9. DOI: 10.1016/j.fluid.2018.03.001.

23. *Frick P.*, *Mandrykin S.*, *Eltishchev V.*, *Kolesnichenko I.* Electro-vortex flows in a cylindrical cell under axial magnetic field. Journal of Fluid Mechanics. 2022. Vol. 949, A–20. DOI: 10.1017/jfm.2022.746.

24. *Losev G.*, *Kolesnichenko I.* The influence of the waveguide on the quality of measurements with ultrasonic Doppler velocimetry. Flow Measurement and Instrumentation. 2020. Vol. 75, no. 101786. DOI: 10.1016/j.flowmeasinst.2020.101786.

25. *Frick P.G.*, *Sokolov D.D.*, *Stepanov R.A.* Wavelets for the space-time structure analysis of physical fields. Physics-Uspekhi. 2022. Vol. 192, no. 1. P. 69–99. DOI: 10.3367/ufne.2020.10.038859.

26. *Vasiliev A.Y.*, *Sukhanovskii A.N.*, *Frick P.G.* Structure and dynamics of large-scale circulation in turbulent convection at high Prandtl number. Fluid Dynamics. 2020. Vol. 55, no. 6. P. 760–767. DOI: 10.31857/S0568528120060134.

Authors' Details:

Poluyanov Alexander Olegovich (corr.); e-mail: poluyanov.a@icmm.ru; ORCID: 0000-0002-6103-5157

Kolesnichenko Ilya Vladimirovich; e-mail: kiv@icmm.ru; ORCID: 0000-0001-9378-5334